Enhanced Four-Body Decays of Charged Higgs Bosons into Off-Shell Pseudoscalar Higgs and $W^\pm$ Boson Pairs in a Lepton-Specific 2-Higgs Doublet Model

Stefano Moretti[a,b] **Muyuan Song**[c]

[a] *School of Physics and Astronomy, University of Southampton, Southampton, SO17 1BJ, United Kingdom*

[b] *Department of Physics and Astronomy, Uppsala University, Box 516, SE-751 20 Uppsala, Sweden*

[c] *Center for High Energy Physics, Peking University, Beijing 100871, China*

E-mail: s.moretti@soton.ac.uk, stefano.moretti@physics.uu.se, muyuansong@pku.edu.cn

ABSTRACT: We study the time-honoured decay $H^\pm \to AW^\pm$ but for the first time, we do so for the case of both A and $W^\pm$ being off-shell, therefore computing a $1 \to 4$ body decay. We show that the corresponding decay rate not only extends the reach of $H^\pm$ searches to small masses of the latter but also that the results of our implementation differ significantly from the yield of the $1 \to 3$ body decay over the phase space region in which the latter is normally used. We show the phenomenological relevance of this implementation in the case of the so-called lepton-specific 2-Higgs Doublet Model (2HDM) over the mass region wherein the aforementioned $1 \to 4$ body decay can dominate just beyond the top (anti)quark mass. This mass region is accessible in the lepton-specific 2HDM as the Yukawa couplings are such that limits from $b \to s\gamma$ and $\tau \to \mu\nu_\tau\bar{\nu}_\mu$ observables on $M_{H^\pm}$ are rather mild. However, we emphasise that similar effects may occur in other 2HDM types, as the $W^\pm H^\mp A$ vertex is 2HDM type independent.

Contents

1 Introduction

The discovery of a neutral Higgs boson in 2012 at the Large Hadron Collider (LHC) has been a significant breakthrough, as such a state (henceforth, denoted by h) is a crucial component of the Standard Model (SM) of particle physics [1, 2]. In fact, the excellent agreement between SM predictions and the subsequent measurements of the h properties (mass, coupling, spin, CP quantum numbers) is a remarkable achievement. In the SM, this particle emerges from a single doublet structure of a complex Higgs field, in which 4 degrees of freedom give rise to the h itself and the longitudinal polarisation component of the $W^\pm$ and Z bosons, following spontaneous Electro-Weak Symmetry Breaking (EWSB), see [3] for a recent review.

However, the possibility of higher Higgs representations, such as more doublets or triplets, with more (pseudo)scalar Higgs states than the discovered one, has not been ruled out yet. Further, notice that the latter can include in their Higgs sector states which have a non-zero Electro-Magnetic (EM) charge, which is of significant interest due to the absence of any spin-zero charged particle in the SM and of theoretical reasons to forbid its existence. Therefore, the production and decay modes resulting from electrically charged interactions involving Higgs bosons can provide a simple way to investigate if any extended structure is underlying the observed Higgs state.

We are concerned here with singly charged Higgs boson state ($H^\pm$), like those belonging to a 2-Higgs Doublet Model (2HDM) [4]. Such an extended Higgs structure is of particular interest as it can be embedded in both Supersymmetry as the Minimal Supersymmetry Standard Model (MSSM) [5–8], and Compositeness, as the Composite 2HDM (C2HDM) [9–12], indeed, two viable theories of the EW scale, i.e., that remedy the hierarchy problem of the SM. In particular, we want to study here the following charged Higgs boson decay: $H^\pm \to AW^\pm$, wherein A is a CP-odd (or pseudoscalar) neutral Higgs state emerging in the 2HDM alongside two more CP-even (or scalar) ones (h and H, with $M_h < M_H$), for a total of 5 of these.

The first studies of $H^\pm \to AW^\pm$ in the context of Supersymmetric models were carried out in Refs. [13, 14], where the $1 \to 2$ and $1 \to 3$ body decay channels were examined in the MSSM. On the Compositeness side, some simple results on this were presented in Ref. [10]. However, a generic treatment of a 2HDM in relation to controlling ensuing Flavour Changing Neutral Currents (FCNCs), as the one afforded in Refs. [4, 15–17], wherein different Yukawa types can eventually be mapped onto the MSSM (a type II) and C2HDM (an aligned type), or indeed other theories, is the most common approach.

In this connection, recent reviews on $H^\pm$ phenomenology in 2HDMs (and beyond) at the Large Hadron Collider (LHC) (and elsewhere) can be found in Refs. [18, 19]. Herein, it has been made clear that, typically, $1 \to 2$ and $1 \to 3$ body decays of the channel $H^\pm \to AW^\pm$ are used in literature, depending on whether $M_{H^\pm} \geq M_A + M_{W^\pm}$ or $M_{H^\pm} < M_A + M_{W^\pm}$, respectively. Even in the most recent phenomenological studies of $H^\pm \to AW^\pm$ decays, found in Refs. [20–22], such a decay mode was studied in these two different kinematic configurations, $1 \to 2$ decays (in a type-II 2HDM) for the former one and $1 \to 3$ body decays (in a type-I 2HDM) in the latter two[1].

In this paper, we revisit these approaches to the computation of $H^\pm \to AW^\pm$ decays, by showing that the $1 \to 3$ one is not the correct extension to the $1 \to 2$ one when $M_{H^\pm} < M_A + M_{W^\pm}$, as we will show that the most appropriate approach is always to compute the $1 \to 4$ body decay, wherein both A and $W^\pm$ can be off-shell (separately or simultaneously). This is true not only when $M_{H^\pm} < \min(M_A, M_{W^\pm})$ but also when $\min(M_A, M_{W^\pm}) < M_{H^\pm} < M_A + M_{W^\pm}$.

To illustrate the phenomenological relevance of our approach at the LHC, we adopt here the so-called lepton-specific 2HDM, as this scenario can afford one with a $H^\pm$ state, which is relatively light (i.e., with a mass comparable to the top (anti)quark mass or lighter) and so is (necessarily) the A state.

The paper is organized as follows. The lepton-specific 2HDM is presented in the next section. We then show the constraints existing from LHC analysis on the $H^\pm \to AW^\pm$ decay in section 3. Our phenomenological analysis of the $1 \to 4$ process, including how it compares to the $1 \to 3$ and $1 \to 2$ ones over the region $M_{H^\pm} > m_t$, is reported upon in section 4, We finally conclude in section 5.

2   Charged Higgs Bosons in the Lepton-Specific 2HDM

In a general 2HDM, the SM is supplemented with two complex $SU(2)_L$ doublets instead of a single one, and these originate two Vacuum Expectation Values (VEVs) obeying the sum rule $v_{\mathrm{SM}} = \sqrt{v_1^2 + v_2^2} = 246$ GeV, as follows:

$$\Phi_i = \begin{pmatrix} \phi_i^+ \\ v_i + \rho_i^0 + I\eta_i^0 \end{pmatrix}, \qquad i = 1, 2. \tag{2.1}$$

---

[1]Notice that, in literature, when computing the $1 \to 3$ body decay, one normally allows for the $W^\pm$ boson being off-shell rather than the A one, as $\Gamma_{W^\pm} \gg \Gamma_A$ over the entire parameter space of popular 2HDMs. (We will come back to this point later.)

The physical charged Higgs states are obtained from mixing the two gauge eigenstates ϕ_1^+ and ϕ_2^+ by a two $\times$ two rotating matrix ($\mathcal{R}$) such that

$$\begin{pmatrix} G^+ \\ H^+ \end{pmatrix} = \mathcal{R} \begin{pmatrix} \phi_1^+ \\ \phi_2^+ \end{pmatrix}, \ \mathcal{R} = \begin{pmatrix} \cos\beta & -\sin\beta \\ \sin\beta & \cos\beta \end{pmatrix}, \tag{2.2}$$

where H^+ is the mass eigenstate and G^+ is the Goldstone mode eaten by $W^\pm$ following EWSB. Here, $\cos\beta$ and $\sin\beta$ can be defined by correlating the two VEVs of the Higgs doublets via $\tan\beta = v_2/v_1$. After rotating the gauge eigenstates into physical states, the charged Higgs Yukawa interactions and those between gauge bosons and charged Higgs states can be expressed as[2]

$$\mathcal{L}_{\text{Yukawa}}^{H^\pm} \supset - \frac{\sqrt{2}V_{ud}}{v_{\text{SM}}} \bar{u} \left(m_u \mathcal{Y}_u^{H^+} P_L + m_d \mathcal{Y}_d^{H^+} P_R \right) d H^+$$
$$- \frac{\sqrt{2}}{v_{\text{SM}}} m_\ell \mathcal{Y}_\ell^{H^+} \bar{\nu}_{\ell L} \ell_R H^+ + \text{h.c.}, \tag{2.3}$$

$$\mathcal{L}_{\text{gauge}}^{H^\pm} \supset + i\frac{g}{2} \left[W_\mu^+ (c_{\beta-\alpha}h - s_{\beta-\alpha}H)\partial^\mu H^- - W_\mu^+ \partial^\mu(c_{\beta-\alpha}h - s_{\beta-\alpha}H)\partial^\mu H^- + \text{h.c.} \right]$$
$$- \frac{g}{2} \left[W_\mu^+ H^- \partial^\mu A - W_\mu^+ \partial^\mu H^- A + \text{h.c.} \right], \tag{2.4}$$

where $u\,(d,\ell)$ represents up (down, lepton) fermions. Here, V_{ud} is the Cabibbo-Kobayashi-Maskawa (CKM) matrix while P_L, P_R are projection operators for left and right-handed spinors, respectively. Furthermore, $\mathcal{Y}_u^{H^+}, \mathcal{Y}_d^{H^+}$ and $\mathcal{Y}_\ell^{H^+}$ are the Yukawa couplings between $H^\pm$ and fermions. The 2HDM without FCNCs [23] can be classified into four types when the multiple scalars do not induce any tree-level contribution due to the presence of an exact Z_2 symmetry: they are named type I, II, lepton-specific (sometimes also called type X or IV) and flipped (sometimes also called type Y or III) [4, 24][3]. The Yukawa couplings $\mathcal{Y}_u^{H^+}$, $\mathcal{Y}_d^{H^+}$ and $\mathcal{Y}_\ell^{H^+}$ in each type of model are characterized by the parameters β, which determines the mixing between the physical states and EW ones (mentioned previously), and α, which determines the mixing in the neutral CP-even (scalar) sector [4, 15, 16]. The values of $\mathcal{Y}_u^{H^+}, \mathcal{Y}_d^{H^+}$ and $\mathcal{Y}_\ell^{H^+}$ are expressed as $\cot\beta$, $-\cot\beta$ and $\tan\beta$, respectively, in the lepton-specific 2HDM [4, 15, 24]. The gauge boson and charged (pseudo)scalar interactions are written in terms of the functions $c_{\beta-\alpha}$ and $s_{\beta-\alpha}$ [25, 26]. Finally, notice that, in contrast to the Yukawa vertices between charged Higgs boson and quarks or leptons, which involves model-dependent values for α and β, the interaction described by the $W^\pm H^\pm A$ vertex is model-independent since it only depends on the EW gauge coupling (g).

3 Searches for Charged Higgs Bosons via $H^\pm \to AW^\pm$

The search for charged Higgs particles via fermionic decay products has been ongoing for several years, encompassing both heavy $(M_{H^\pm} > m_t)$ and light $(M_{H^\pm} < m_t)$ states. In the

---

[2]Hereafter, we use the short-hand notations $\cos X \equiv c_X$ and $\sin X \equiv s_X$.

[3]In the aligned 2HDM, FCNCs via Higgs boson exchanges at tree-level vanish due to the assumption that one of the Yukawa matrices for each charged fermion is proportional to the other.

search for heavier states, the ATLAS [27–29] and CMS [30–34] collaborations have focused on charged Higgs particles yielding top and bottom final states, collected at collider energies ranging from 8 TeV to 13 TeV. In terms of the gauge boson scalar mixing, ATLAS explored $W^{\pm}Z$ final states [35] at $\sqrt{s} = 8$ TeV, while CMS conducted the exact search at $\sqrt{s} = 13$ TeV [36]. For masses below the top quark one, both hadronic and leptonic channels have been investigated by Tevatron, LEP, and LHC searches. (Some of these searches have been reviewed in Ref. [37].) The D0 and CDF collaborations at Tevatron performed a search for the process $p\bar{p} \to t\bar{t}$ where one top (anti)quark decays to $H^{\pm}b$ at $\sqrt{s} = 1.96$ TeV. The D0 collaboration searched for disappearance modes with both leptonic and hadronic final states while the CDF collaboration tested the specific appearance mode $H^{\pm} \to cs$ in the mass range 80–90 GeV [38, 39]. The LEP groups ALEPH, DELPHI, L3 and OPAL finalised a combined analysis at $\sqrt{s} = 189 - 209$ GeV for $H^{\pm}$ decays via fermionic decay modes assuming $\mathrm{BR}(H^{\pm} \to \mathrm{hadrons}) + \mathrm{BR}(H^{\pm} \to \mathrm{leptons}) = 1$. Eventually, LHC searches extended the mass limit on $H^{\pm}$ to close to m_t for most such modes. A study of leptonic decay modes of $H^{\pm}$ states, with dominant $\tau\nu$ signatures, has been performed at $\sqrt{s} = 7, 8$ and 13 TeV in both ATLAS and CMS from $pp \to t\bar{t}$ followed by $t \to H^{\pm}b$ [28, 30–32, 40–43]. For hadronic (di-jet) modes, the CMS collaboration searched for charged Higgs bosons decaying into cs and cb over different mass ranges at different centre-of-mass energies. For $H^{\pm} \to cs$, searches were carried out at $\sqrt{s} = 8$ TeV ($L = 19.7$ fb^{-1}) for $M_{H^{\pm}}$ in the range 90 to 160 GeV [44] and at $\sqrt{s} = 13$ TeV ($L = 35.9$ fb^{-1}) for $M_{H^{\pm}}$ between 80 and 160 GeV [45], assuming a full cs decay mode with an exclusion limit for $\mathrm{BR}(t \to H^{\pm}b)$ ranging from 1.68% to 0.25%. For $H^{\pm} \to cb$, CMS searched the region $M_{H^{\pm}}$ from 90 to 150 GeV at $\sqrt{s} = 8$ TeV [46]. Furthermore, the ATLAS collaboration [47] conducted their first $H^{\pm} \to cs$ search at $\sqrt{s} = 7$ TeV in 2011 for $M_{H^{\pm}}$ up to 150 GeV and later, using data from 2015 to 2018 with an integrated luminosity of 139 fb^{-1}, at $\sqrt{s} = 13$ TeV [48], performed an analysis of light charged Higgs boson production from (anti)top quark decays followed by $H^{\pm} \to cb$ with $60 \leq M_{H^{\pm}} \leq 160$ GeV, quite recently. This search obtained a local 3σ (estimating a global 2.5σ) excess for $M_{H^{\pm}} = 130$ GeV based on neural network for $b-$jet tagging identification. In short, despite various experiments exploring all the above search channels for charged Higgs particles, those with mixed gauge and Higgs boson final states, specifically $AW^{\pm}$ ones, have not received comparable attention. Therefore, we illustrate these in some detail here.

Previous $AW^{\pm}$ searches at electron-positron colliders (like LEP) [49], via $e^+e^- \to H^+H^-$, focused on the type I 2HDM with $M_{H^{\pm}}$ up to half the collider energy with M_A ranging from 10 to 70 GeV. In 2019, the CMS collaboration investigated the first search for $H^{\pm}$ decay to $AW^{\pm}$ in a pp collider. The search was carried out at $\sqrt{s} = 13$ TeV with an integrated luminosity of 35.9 fb^{-1} [50]. Upper limits on $H^{\pm}$ decay rates for a charged Higgs $H^{\pm}$ range from 100 to 160 GeV were determined for three lepton final states ($e\mu\mu$ or $\mu\mu\mu$) with M_A ranging from 15 to 75 GeV. The product of $\mathrm{BR}(t \to H^{\pm}b) \times \mathrm{BR}(H^{\pm} \to AW^{\pm}) \times \mathrm{BR}(A \to \mu^+\mu^-)$ was limited to be between 1.9×10^{-6} to 8.9×10^{-6} at 95% Confidence Level (CL). Furthermore, the CMS collaboration recently conducted the first search for a heavy charge state decaying into a heavy neutral Higgs (i.e., H, with a mass M_H larger than m_t) and a $W^{\pm}$ boson [51]. It took place with $\sqrt{s} = 13$ TeV and used data from 2016-2018

with an integrated luminosity of $L = 138$ fb^{-1}. The upper limits for the product of $\sigma_{H^\pm}$ and BR$(H^\pm \to HW^\pm) \times$ BR$(H \to \tau^+\tau^-)$ were obtained from 0.085 pb to 0.019 pb for $M_{H^\pm}$ between 300 and 700 GeV. The only preliminary search by the ATLAS for the decay of $H^\pm$ into a $W^\pm$ gauge boson and a pseudoscalar A state, with A decaying into $\mu^+\mu^-$, was conducted at $\sqrt{s} = 13$ TeV ($L = 139$ fb^{-1}) in 2021 [52]. The analysis was performed for $M_{H^\pm}$ values of 120, 140, and 160 GeV, with M_A ranging from 15 to 75 GeV, and the product of BR$(t \to H^\pm b) \times$ BR$(H^\pm \to AW^\pm) \times$ BR$(A \to \mu^+\mu^-)$ was used to determine the observed exclusion limits of 0.9 to 6.9×10^{-6} (with expected limits ranging from 1.6 to 9.9×10^{-6}).

Before closing this section, we emphasise that all our numerical results will be presented for parameter space points of the lepton-specific 2HDM that are compliant with the above limits (relative to the $H^\pm$ sector), specifically being consistent with the outputs of HiggsBounds [53], which also produces limits on the neutral Higgs sector (to which we have also adhered). Furthermore, the same constraints implemented in HiggsSignals [54], applied to our h state (with mass $M_h = 125$ GeV), were also accounted for. Finally, we have checked that flavour limits are also correctly considered, complying with the [55] outputs.

4 Phenomenology of $H^\pm \to AW^\pm$ Decays at the LHC

The dominant charged Higgs production mechanism at the LHC in our scenario would mainly occur via $gg, q\bar{q} \to t\bar{b}H^-$, which Feynman diagrams are illustrated in Fig. 1 (for other less significant channels for producing a charged Higgs boson at the LHC, see Ref. [57]). As explained in [56] they can be used for $H^\pm$ production, whichever mass suits our purposes as we will be scanning $M_{H^\pm}$ values around and just beyond m_t. Their implementation in CalcHEP [58] has been tested (for the MSSM case) against the explicit formulae given in Refs. [59, 60] and deployed for the computation in the lepton-specific 2HDM, for which we have created a dedicated model file.

Although we are focusing on the $AW^\pm$ channel in $H^\pm$ decays, the fermionic ones, mainly $\tau\nu$, cs, cb and tb, constitute channels with significant BR, especially the first (as we are in the lepton-specific 2HDM) and last (because of the generally strong Yukawa couplings), which can be dominant over $AW^\pm$, depending on the values of $M_{H^\pm}$ and the other parameters of our scenario[4].

Since the $H^\pm AW^\pm$ vertex is model-independent as it only depends on the EW coupling (g), the tree-level expression for the on-shell $H^\pm \to AW^\pm$ $(1 \to 2$ body) decay width, illustrated in the left panel of Fig. 2 (where $M_{H^\pm} \gg M_A + M_{W^\pm}$), can be expressed as follows [13, 14, 61]:

$$\Gamma_{H^\pm \to AW^\pm} = \frac{G_F}{8\sqrt{2}\pi} \frac{M_{W^\pm}^4}{M_{H^\pm}} \lambda^{\frac{1}{2}}(M_A^2, M_{W^\pm}^2; M_{H^\pm}^2) \lambda(M_A^2, M_{H^\pm}^2; M_{W^\pm}^2),$$
$$\lambda(x, y; z) = (1 - \frac{x}{z} - \frac{y}{z})^2 - \frac{4xy}{z^2}, \tag{4.1}$$

---

[4]To simplify the numerical treatment of the $H^\pm$ decay phenomenology, we will take $M_H \gg M_{H^\pm}$. In contrast, the decay of $H^\pm \to hW^\pm$ can generally be neglected as the $W^\pm H^\mp h$ coupling is extremely small.
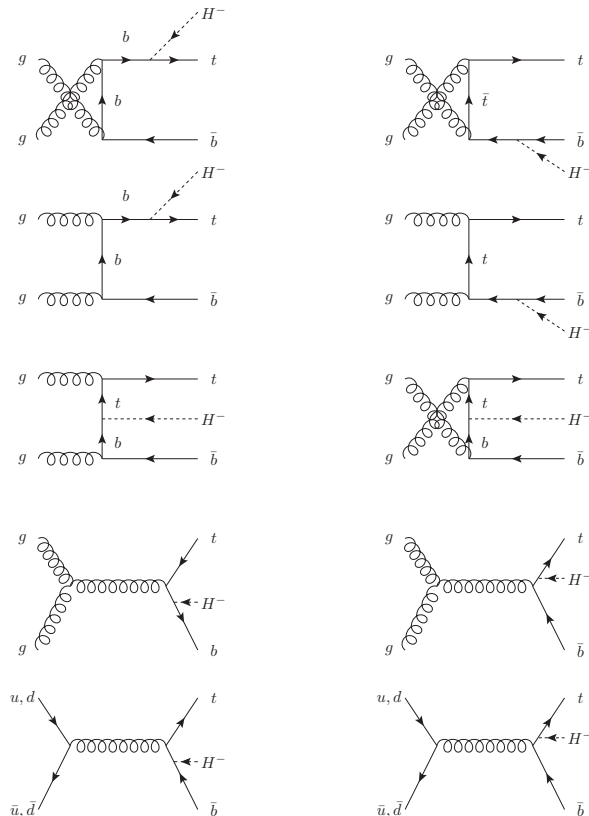
Figure 1. Feynman diagrams for gg (top 8 graphs) and $q\bar{q}$ (bottom 2 graphs) induced production of the $t\bar{b}H^-$ final state, applicable to both cases $M_{H^\pm} < m_t$ and $M_{H^\pm} > m_t$ (see Ref. [56]).

where G_F is Fermi constant, $M_{H^\pm}, M_A$ and $M_{W^\pm}$ are the masses of the charged Higgs boson, pseudoscalar Higgs boson and $W^\pm$ boson, respectively. The aforementioned result would not hold if $M_{H^\pm} < M_A + M_{W^\pm}$. In this case, the $(1 \to 3$ body) decay $H^\pm \to AW^{\pm *}$ would open, wherein the gauge boson is off-shell, which subsequently decays into light fermions like in the centre panel of Fig. 2. One method to compute the corresponding decay width is to integrate the corresponding Dalitz plot density of the process, which can
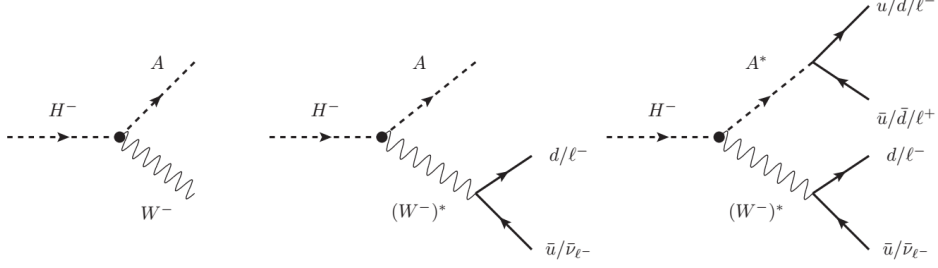
Figure 2. Feynman diagrams for on shell $H^- \to AW^-$ process (left panel), three-body $H^- \to A(W^-)^*$ process (centre panel) and four body $H^- \to A^*(W^-)^*$ process with fermionic final states only (right panel). When $M_A > M_Z$, there exists a subdiagram $A \to Z\gamma$ in the top part of the right panel, which is not presented in this diagram.

be expressed as follows [14, 61]:

$$\Gamma_{H^\pm \to AW^{\pm *} \to Af\bar{f}} = \frac{9G_F^2 M_{W^\pm}^4}{16\pi^3} \int_{1-x_2-k_A}^{1-\frac{k_A}{1-x_2}} dx_1 \int_0^{1-k_A} dx_2 F_{AW},$$

$$F_{AW} = \frac{(1-x_1)(1-x_2) - k_A}{(1-x_1-x_2-k_A+k_W)^2 + k_W\gamma_{W^\pm}},$$

$$k_A = \frac{M_A^2}{M_{H^\pm}^2}, \ k_W = \frac{M_{W^\pm}^2}{M_{H^\pm}^2}, \ \gamma_W = \frac{\Gamma_{W^\pm}^2}{M_{H^\pm}^2}, \tag{4.2}$$

where $M_{H^\pm}$, M_A and $M_{W^\pm}$ are the relevant particle masses and $\Gamma_{W^\pm}$ is the width of the $W^\pm$ boson. The integration variables (x_1, x_2) correspond to the energy of the final states emerging from the virtual $W^\pm$ and are expressed as $x_{1,2} = 2E_{1,2}/M_{H^\pm}$. In fact, one should also account for the other $1 \to 3$ body decay, i.e., $H^\pm \to A^*W^\pm$, where the Higgs boson contribution should be accounted for through the h decay currents, which we have done. However, as expected, the corresponding contribution to the partial decay width is generally small, though altogether not negligible, with the A width of $\mathcal{O}(\mathrm{GeV})$.

When the charged Higgs boson is lighter than both A and $W^\pm$, then the $1 \to 4$ body decay mode should be computed, $H^\pm \to A^*W^{\pm *}$, where both A and $W^\pm$ are off-shell and described by currents (as shown in the right panel of the Fig. 2). The ensuing partial width

can be calculated through a double invariant mass squared integral [13, 61–63],

$$
\begin{aligned}
\Gamma_{H^\pm \to A^*(W^\pm)^*} &= \int_0^{M_{H^\pm}^2} \frac{dq_A^2 M_A \Gamma_A}{\pi[(q_A^2 - M_A^2)^2 + (M_A \Gamma_A)^2]} \\
&\times \int_0^{(M_{H^\pm} - q_A)^2} \frac{dq_{W^\pm}^2 M_{W^\pm} \Gamma_{W^\pm}}{\pi[(q_{W^\pm}^2 - M_{W^\pm}^2)^2 + (M_{W^\pm} \Gamma_W^\pm)^2]} \\
&\times \frac{G_F}{8\sqrt{2}\pi} \frac{M_{W^\pm}^4}{M_{H^\pm}} \sqrt{(1 - \frac{q_A^2}{M_{H^\pm}^2} - \frac{q_{W^\pm}^2}{M_{H^\pm}^2})^2 - \frac{4q_A^2 q_{W^\pm}^2}{M_{H^\pm}^4}} \\
&\times \left[(1 - \frac{M_A^2}{q_{W^\pm}^2} - \frac{M_{H^\pm}^2}{q_{W^\pm}^2})^2 - \frac{4M_A^2 M_{H^\pm}^2}{q_{W^\pm}^4} \right],
\end{aligned}
\tag{4.3}
$$

where $q_A^2, q_{W^\pm}^2$ are the (virtual) invariant masses squared of A and $W^\pm$, with Γ_A and $\Gamma_{W^\pm}$ the corresponding total widths. The two fractions within the formula, which contain $M_x \Gamma_x$ $(x = A, W^\pm)$, are nothing but the well-known Breit-Wigner formulae.

All these $1 \to 2$, $1 \to 3$, and $1 \to 4$ decays are calculated through a Mathematica notebook [64]. The uncertainty in our results is proportional to $1/\sqrt{N}$, where N is the number of evaluations performed. The uncertainty of results would reduce for a large number of N. To remove fluctuations and capture all relevant physics features, we have used $N = 2000000$ as default throughout so that our predictions are essentially (numerical) error-free. To obtain our final $1 \to 4$ body results, we had to compute the total decay width of the pseudoscalar A state, for which we utilized the formulae provided in Appendix A of Ref. [24]. The total width of the A state, Γ_A, includes the tree-level decays to $q\bar{q}$ ($q = s, c$ and b) and $\ell\bar{\ell}$ ($\ell = \mu$ and τ) as well as the one-loop decays to gg and $\gamma\gamma$. For A masses greater than that of the Z boson, the decay $A \to Z\gamma$ must also be considered. We utilized the equations presented in Ref. [61] to compute the on-shell decays of the heavy-charged Higgs to the top and bottom quarks and the lepton/light quark modes. However, since our interest lies in the $H^\pm$ mass range from m_t to approximately 220 GeV, we also computed the $1 \to 3$ body decay $H^\pm \to bt^*$, where the top (anti)quark is off-shell. To do so, we employed the formulae in eqs. (63)-(64) of Ref. [61], which used the Dalitz plot density of the $H^\pm \to bt^*$ process to compute the integral with off-shell t decays to $W^\pm b$. To facilitate a comparison between the analytic formula, which integrates the energy of substates (from off-shell t or $\bar{t}$) out, and the exact integral form (where only m_b is neglected due to its smallness compared to the energy $E_{b(\bar{b})}$), we observed a typo in the analytical expression for the $1 \to 3$ body decay. Specifically, we had to omit the extra factor of $1/2$ in front of eq. (65). Therefore, we implemented the above formulae but with such a correction to obtain both on-shell ($1 \to 2$) and off-shell ($1 \to 3$) results for the BR($H^\pm \to t^{(*)}b$) while achieving agreement with the fully numerical results of Ref. [13].

As intimated, in this study, the charged Higgs boson is kept lighter than the heavy neutral scalar state, H, to avoid additional contributions from the decay $H^\pm \to HW^\pm$ [65, 66]. Furthermore, in the alignment limit [67–69], where the lightest physical Higgs state of our lepton-specific 2HDM is identical to the SM Higgs boson (i.e., $h \equiv h_{\rm SM}$), the fact that $s_{\beta-\alpha} = 1$ would forbid the $H^\pm \to hW^\pm$ decay at tree-level. Therefore, the $H^\pm$ bosonic
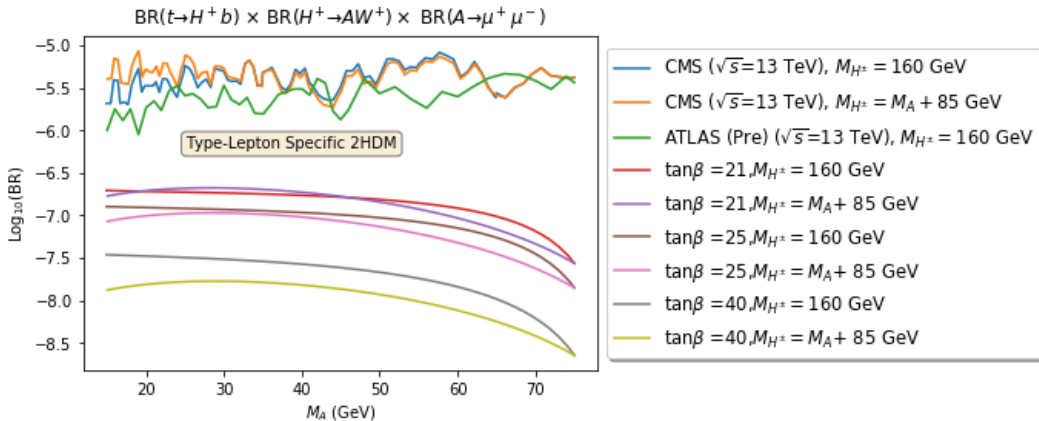
Figure 3. The exclusion bounds for the BR product in eq. (4.4) from CMS data with $\sqrt{s} = 13$ TeV and $L = 35.9$ fb^{-1} [50] in the range of M_A between 15 and 75 GeV. For the blue line we have $M_{H^\pm} = 160$ GeV while for the orange line we have $M_{H^\pm} = M_A + 85$ GeV. The green solid line represents the upper bound from a preliminary ATLAS search (using $\sqrt{s} = 13$ TeV and $L = 139$ fb^{-1}) with $M_{H^\pm} = 160$ GeV [52]. Three BPs ($\tan\beta = 21, 25, 40$) in the lepton-specific 2HDM are plotted with respective colours as in the legend, and the BR results (Y-axis) are shown in the logarithmic scale with base 10.

decay channel with a $W^\pm$ in the final state only involves the pseudoscalar Higgs boson A, as we further ignore the $\gamma W^\pm$ and $ZW^\pm$ decays, since they are one-loop suppressed.

The current experimental limits from the $H^\pm \to AW^\pm$ search are given on the following product,

$$\text{BR}(t \to H^\pm b) \times \text{BR}(H^\pm \to AW^\pm) \times \text{BR}(A \to \mu^+\mu^-), \tag{4.4}$$

where di-muon decays of the A state are pursued. This is a rather sensible signature to adopt in the lepton-specific 2HDM, wherein leptonic decays of the Higgs state are generically enhanced (with respect to other 2HDM types), further recalling the efficient identification of muons and the relative cleanliness of signatures containing them. We use two experimental analyses here, a published CMS one ($\sqrt{s} = 13$ TeV and $L = 35.9$ fb^{-1} [50]) and a preliminary ATLAS one ($\sqrt{s} = 13$ TeV and $L = 139$ fb^{-1} [52]). The corresponding limits on the above product of BRs are shown in Fig. 3. In order to compare the viability of the lepton-specific 2HDM against such data, we have chosen here three Benchmark Points (BPs), with $\tan\beta = 20, 21$ and 40. For the same choice of charged Higgs masses adopted by the experimental collaborations, i.e., $M_{H^\pm} = 160$ GeV (blue line) and $M_{H^\pm} = M_A + 85$ GeV (orange line), we see that they are indeed compliant with data. We further note that when $\tan\beta$ is small (~ 8 or less), the BR product in eq. (4.4) will be excluded for the lepton-specific 2HDM due to the large values of the BR($t \to H^\pm b$). This is because the Yukawa couplings between the top and bottom (anti)quarks with the charged Higgs boson are inversely proportional to $\tan\beta$, leading to the general result of smaller values of $\tan\beta$ being more strongly constrained by current bounds. Furthermore, the low energy observables associated with $b \to s\gamma$ and $\tau \to \mu\bar{\nu}\nu$ transitions can also limit values of $M_{H^\pm}$ and

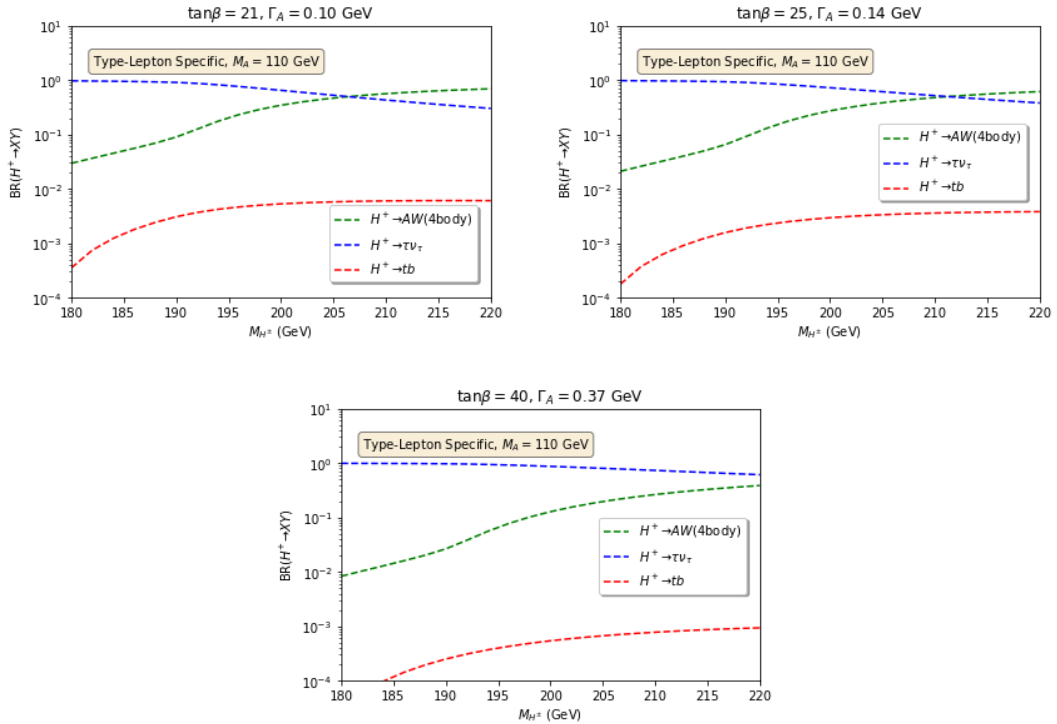**Figure 4.** BR($H^{\pm} \to XY$) as a function of $M_{H^{\pm}}$ with $M_A = 110$ GeV and $\tan\beta = 21, 25$ and 40 (top-left, top-right and bottom frame, respectively). Here, X and Y correspond to three different decays of the $H^{\pm}$ state. In each subplot, the blue dashed line represents the BR($H^{\pm} \to \tau\nu_{\tau}$), the green dashed line relates to the BR($H^{\pm} \to A^*W^{\pm*}$) while the red dashed line corresponds to the BR($H^{\pm} \to tb$). Other decay channels ($cs, cb, ...$) have BRs below $\mathcal{O}(10^{-4})$ (i.e., they are not relevant phenomenologically) and thus are not presented here.

$\tan\beta$ in the lepton-specific 2HDM. Concerning the former, unlike the case of type II and flipped 2HDM, where $M_{H^{\pm}}$ is required to be above 600 GeV or so, in the lepton-specific case only the following milder constraint applies: $M_{H^{\pm}} > 100$ GeV with $\tan\beta > 5$ [24]. Concerning the latter, the decay $\tau \to \mu\bar{\nu}\nu$ imposes constraints on $\tan\beta$ such that, in our scenario, values of it greater than 20 and 40 would require $H^{\pm}$ to have a mass greater than 80 and 120 GeV, respectively. Thus, the three BPs chosen for our study evade these constraints too.

In Fig. 4, the phenomenologically relevant decays of charged Higgs bosons (e.g., with BRs larger than $\mathcal{O}(10^{-4})$) in the lepton-specific 2HDM are presented, in the mass region 180 GeV $< M_{H^{\pm}} <$ 220 GeV for $M_A = 110$ GeV. Herein, the $1 \to 4$ body decay is used to estimate the BR($H^{\pm} \to A^*W^{\pm*}$). From these results, it is clear that $\tau\nu_{\tau}$ decays generally dominate over tb ones, and this pattern is obviously because our BPs have rather large values of $\tan\beta$, which then enhance the former and deplete the latter. However, it is remarkable to notice that $A^*W^{\pm*}$ decays can be very large, the more so, the bigger $M_{H^{\pm}}$ and the smaller $\tan\beta$ so that at times they can dominate the $H^{\pm}$ decay phenomenology. It is therefore important to see whether these parameter space regions of the lepton-specific 2HDM can become observable through this channel in the near future and,
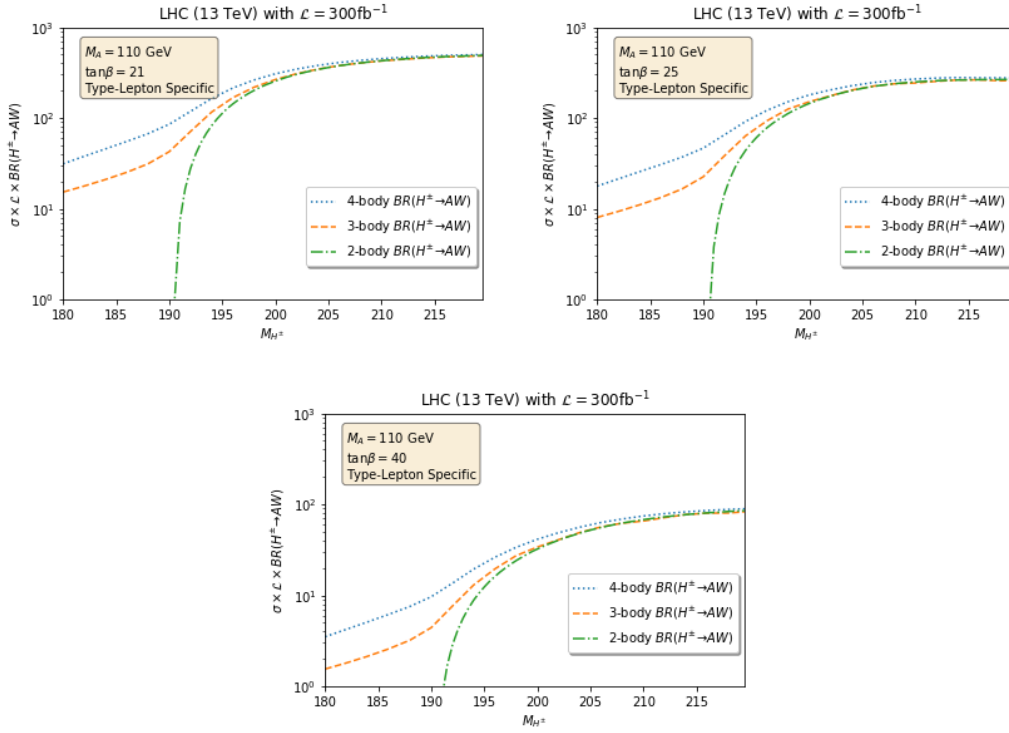
Figure 5. Event rates as per eq. (4.5) at $\sqrt{s} = 13$ TeV as function of $M_{H^\pm}$ with $M_A = 110$ GeV and $\tan\beta = 21, 25$ and 40 (top-left, top-right and bottom frame, respectively). Herein, the $\mathrm{BR}(H^\pm \to A^{(*)}W^{\pm(*)})$ is computed as follows: the blue dotted line represents the $1 \to 4$ body case; the orange dashed line represents the $1 \to 3$ body case, while the green dashed-dot line represents the $1 \to 2$ body case.

crucially, whether correspondingly the $1 \to 4$ body formulation of our target decay differs from the $1 \to 3$ and $1 \to 2$ ones. In fact, notice that the $H^\pm$ mass region explored in this figure is the one where both of the latter are normally used: the $1 \to 2$ body decay for $M_{H^\pm} > M_A + M_{W^\pm} \approx 190$ GeV and the $1 \to 3$ one otherwise.

With an increase in integrated luminosity up to 300 fb^{-1} achievable by both ATLAS and CMS in Run 3 of the LHC [70], the number of expected $H^\pm \to A^{(*)}W^{\pm(*)}$ signal events can be expressed as a cross-section times BR times L product, as follows:

$$\sigma(gg\, q\bar{q} \to t\bar{b}H^- + \text{c.c.}) \times \mathrm{BR}(H^\pm \to AW) \times L(= 300 \text{ fb}^{-1}). \tag{4.5}$$

The above expression is plotted in in Fig. 5 as a function of $M_{H^\pm}$ over the usual interval, for the M_A and $\tan\beta$ choices already mentioned, considering $1 \to 2$ body (green dashed-dot line), $1 \to 3$ body (orange dashed line) and $1 \to 4$ body (blue dotted line) decays in the computation of $\mathrm{BR}(H^\pm \to A^{(*)}W^{\pm(*)})$. If $M_{H^\pm}$ is less than $M_A + M_{W^\pm}$, the $1 \to 2$ body decay process shuts off sharply, and no events can be generated. Here, the $1 \to 3$ body and $1 \to 4$ body decay results are non-zero, as expected, but the two start differing already at 220 GeV or so, with such a difference growing more and more as $M_{H^\pm}$ diminishes. Remarkably, the $1 \to 4$ body results differ drastically from the $1 \to 3$ one below 190

$M_{H^\pm}$ (GeV)	$1 \to 2$	$1 \to 3$	$1 \to 4$
180	0	1	3
190	0	4	9
200	32	33	41
210	67	67	74
218	83	83	89

Table 1. Event rates as per eq. (4.5) at $\sqrt{s} = 13$ TeV for sample values of $M_{H^\pm}$, with $M_A = 110$ GeV and $\tan\beta = 40$, depending on whether $1 \to 2$, $1 \to 3$ or $1 \to 4$ body decays are used in the computation of $\mathrm{BR}(H^\pm \to A^{(*)}W^{\pm(*)})$. The event numbers are rounded to the nearest integer.

GeV, well over a factor of two excess. We make this manifest in Tab. 1, where the above expression is given for $M_A = 110$ GeV, $\tan\beta = 40$ and in correspondence of the following choices of charged Higgs boson mass: $M_{H^\pm} = 180$, 190, 200, 210 and 218 GeV.

5 Conclusions

In summary, we have shown how the modelling of the decay of a charged Higgs boson $H^\pm$ into a pseudoscalar Higgs state A and a $W^\pm$ gauge boson, below the threshold for on-shell $AW^\pm$ production, depends strongly upon how the off-shellness of either or both the A and $W^\pm$ states is accounted for. The naive expectation that the $1 \to 3$ body decay is appropriate for the description of the mass region $\min(M_A, M_{W^\pm}) < M_{H^\pm} < M_A + M_{W^\pm}$, wherein the dominant contribution typically comes from $AW^{\pm*}$ (the $A^*W^\pm$ channel is typically subleading as in most viable model realisations embedding such a decay one has $\Gamma_A \ll \Gamma_{W^\pm}$), appears to be incorrect in the presence of a complete $1 \to 4$ body computation, i.e., $H^\pm \to A^*W^{\pm*}$, which yields substantially larger rates than the $1 \to 3$ body description in the above $H^\pm$ mass region.

These results are general, but we have illustrated them for a specific realisation of the minimal Higgs sector construct, which enables the aforementioned decays, i.e., a 2HDM. Specifically, we have chosen the so-called lepton-specific realisation of it for the following reasons. Firstly, it is one for which experimental searches at the LHC have sensitivity, if anything, because these tend to exploit relatively clean signatures involving leptons (chiefly, muons) amid the overwhelming QCD background of the LHC, which are in turn generally enhanced in the 2HDM realisation chosen. Secondly, the $H^\pm \to A^{(*)}W^{\pm(*)}$ decay (when accompanied by $gg, q\bar{q} \to t\bar{b}H^- +$ c.c. production) can be phenomenologically relevant at the LHC over a substantial region of the lepton-specific 2HDM, where $\tan\beta$ is large (more than 8 or so) and $M_{H^\pm}$ is rather small (just below or above the top (anti)quark mass). Thirdly, while such configurations of this model are currently compliant with LHC data from Run 1 and 2, which have revealed no excess in this channel, they could potentially become observable at Run 3, as event rates in the presence of a $1 \to 4$ body description of the discussed decay can be up to a factor of 2 or so larger than the $1 \to 3$ body ones, thereby making $H^\pm \to A^*W^{\pm*}$ decays a promising area of investigation for future LHC analyses.

As an outlook element, we should finish by emphasising that we have not tested yet the discussed $1 \rightarrow 4$ body decay in its natural region of validity, i.e., when $M_{H^\pm} \leq \min(M_A, M_{W^\pm})$, which we will do in a forthcoming publication, in the very low mass region of both the $H^\pm$ and A states in the context of a type I 2HDM.

Acknowledgments

References

[1] ATLAS collaboration, *Observation of a new particle in the search for the Standard Model Higgs boson with the ATLAS detector at the LHC*, *Phys. Lett. B* **716** (2012) 1 [`1207.7214`].

[2] CMS collaboration, *Observation of a New Boson at a Mass of 125 GeV with the CMS Experiment at the LHC*, *Phys. Lett. B* **716** (2012) 30 [`1207.7235`].

[3] S. Khalil and S. Moretti, *Standard Model Phenomenology*, CRC Press (6, 2022).

[4] G.C. Branco, P.M. Ferreira, L. Lavoura, M.N. Rebelo, M. Sher and J.P. Silva, *Theory and phenomenology of two-Higgs-doublet models*, *Phys. Rept.* **516** (2012) 1 [`1106.0034`].

[5] S. Moretti and S. Khalil, *Supersymmetry Beyond Minimality: From Theory to Experiment*, CRC Press (2019).

[6] S.P. Martin, *A Supersymmetry primer*, *Adv. Ser. Direct. High Energy Phys.* **18** (1998) 1 [`hep-ph/9709356`].

[7] A. Salam and J.A. Strathdee, *Supergauge Transformations*, *Nucl. Phys. B* **76** (1974) 477.

[8] S. Ferrara, J. Wess and B. Zumino, *Supergauge Multiplets and Superfields*, *Phys. Lett. B* **51** (1974) 239.

[9] J. Mrazek, A. Pomarol, R. Rattazzi, M. Redi, J. Serra and A. Wulzer, *The Other Natural Two Higgs Doublet Model*, *Nucl. Phys. B* **853** (2011) 1 [`1105.5403`].

[10] S. De Curtis, L. Delle Rose, S. Moretti and K. Yagyu, *A Concrete Composite 2-Higgs Doublet Model*, *JHEP* **12** (2018) 051 [`1810.06465`].

[11] S. De Curtis, L. Delle Rose, S. Moretti and K. Yagyu, *A Composite 2-Higgs Doublet Model*, *PoS* **EPS-HEP2019** (2020) 344 [`1910.13699`].

[12] S. De Curtis, S. Moretti, R. Nagai and K. Yagyu, *CP-Violation in a composite 2-Higgs doublet model*, *JHEP* **10** (2021) 040 [`2107.08201`].

[13] S. Moretti and W.J. Stirling, *Contributions of below threshold decays to MSSM Higgs branching ratios*, *Phys. Lett. B* **347** (1995) 291 [`hep-ph/9412209`].

[14] A. Djouadi, *The Anatomy of electro-weak symmetry breaking. II. The Higgs bosons in the minimal supersymmetric model*, *Phys. Rept.* **459** (2008) 1 [`hep-ph/0503173`].

[15] J.F. Gunion, H.E. Haber, G.L. Kane and S. Dawson, *The Higgs Hunter's Guide*, vol. 80, CRC Press (2000).

[16] J.F. Gunion, H.E. Haber, G.L. Kane and S. Dawson, *Errata for the Higgs hunter's guide*, hep-ph/9302272.

[17] A. Pich and P. Tuzon, *Yukawa Alignment in the Two-Higgs-Doublet Model*, *Phys. Rev. D* **80** (2009) 091702 [0908.1554].

[18] A.G. Akeroyd et al., *Prospects for charged Higgs searches at the LHC*, *Eur. Phys. J. C* **77** (2017) 276 [1607.01320].

[19] A. Arhrib, R. Benbrik, H. Harouiz, S. Moretti and A. Rouchad, *A Guidebook to Hunting Charged Higgs Bosons at the LHC*, *Front. in Phys.* **8** (2020) 39 [1810.09106].

[20] F. Kling, A. Pyarelal and S. Su, *Light Charged Higgs Bosons to AW/HW via Top Decay*, *JHEP* **11** (2015) 051 [1504.06624].

[21] A. Arhrib, R. Benbrik and S. Moretti, *Bosonic Decays of Charged Higgs Bosons in a 2HDM Type-I*, *Eur. Phys. J. C* **77** (2017) 621 [1607.02402].

[22] A. Arhrib, R. Benbrik, H. Harouiz, S. Moretti, Y. Wang and Q.-S. Yan, *Implications of a light charged Higgs boson at the LHC run III in the 2HDM*, *Phys. Rev. D* **102** (2020) 115040 [2003.11108].

[23] V.D. Barger, J.L. Hewett and R.J.N. Phillips, *New Constraints on the Charged Higgs Sector in Two Higgs Doublet Models*, *Phys. Rev. D* **41** (1990) 3421.

[24] M. Aoki, S. Kanemura, K. Tsumura and K. Yagyu, *Models of Yukawa interaction in the two Higgs doublet model, and their collider phenomenology*, *Phys. Rev. D* **80** (2009) 015017 [0902.4665].

[25] S.L. Glashow and S. Weinberg, *Natural Conservation Laws for Neutral Currents*, *Phys. Rev. D* **15** (1977) 1958.

[26] E.A. Paschos, *Diagonal Neutral Currents*, *Phys. Rev. D* **15** (1977) 1966.

[27] ATLAS collaboration, *Search for charged Higgs bosons decaying into top and bottom quarks at $\sqrt{s}$ = 13 TeV with the ATLAS detector*, *JHEP* **11** (2018) 085 [1808.03599].

[28] ATLAS collaboration, *Search for charged Higgs bosons decaying via $H^{\pm} \to \tau^{\pm}\nu_{\tau}$ in the τ+jets and τ+lepton final states with 36 fb^{-1} of pp collision data recorded at $\sqrt{s}$ = 13 TeV with the ATLAS experiment*, *JHEP* **09** (2018) 139 [1807.07915].

[29] ATLAS collaboration, *Search for charged Higgs bosons decaying into a top quark and a bottom quark at $\sqrt{s}$ = 13 TeV with the ATLAS detector*, *JHEP* **06** (2021) 145 [2102.10076].

[30] CMS collaboration, *Search for a charged Higgs boson in pp collisions at $\sqrt{s}$ = 8 TeV*, *JHEP* **11** (2015) 018 [1508.07774].

[31] CMS collaboration, *Search for charged Higgs bosons with the $H^{\pm} \to \tau^{\pm}\nu_{\tau}$ decay channel in the fully hadronic final state at $\sqrt{s}$ = 13 TeV*, CMS-PAS-HIG-16-031.

[32] CMS collaboration, *Search for charged Higgs bosons in the $H^{\pm} \to \tau^{\pm}\nu_{\tau}$ decay channel in proton-proton collisions at $\sqrt{s}$ = 13 TeV*, *JHEP* **07** (2019) 142 [1903.04560].

[33] CMS collaboration, *Search for a charged Higgs boson decaying into top and bottom quarks in events with electrons or muons in proton-proton collisions at $\sqrt{s}$ = 13 TeV*, *JHEP* **01** (2020) 096 [1908.09206].

[34] CMS collaboration, *Search for charged Higgs bosons decaying into a top and a bottom quark in the all-jet final state of pp collisions at $\sqrt{s}$ = 13 TeV*, *JHEP* **07** (2020) 126 [2001.07763].

[35] ATLAS collaboration, *Search for a Charged Higgs Boson Produced in the Vector-Boson Fusion Mode with Decay $H^{\pm} \to W^{\pm}Z$ using pp Collisions at $\sqrt{s}$ = 8 TeV with the ATLAS Experiment*, *Phys. Rev. Lett.* **114** (2015) 231801 [1503.04233].

[36] CMS collaboration, *Search for Charged Higgs Bosons Produced via Vector Boson Fusion and Decaying into a Pair of W and Z Bosons Using pp Collisions at $\sqrt{s}$ = 13 TeV*, *Phys. Rev. Lett.* **119** (2017) 141802 [1705.02942].

[37] A.G. Akeroyd, S. Moretti and M. Song, *Light charged Higgs boson with dominant decay to quarks and its search at the LHC and future colliders*, *Phys. Rev. D* **98** (2018) 115024 [1810.05403].

[38] D0 collaboration, *Search for Charged Higgs Bosons in Top Quark Decays*, *Phys. Lett. B* **682** (2009) 278 [0908.1811].

[39] CDF collaboration, *Search for charged Higgs bosons in decays of top quarks in p$\bar{p}$ collisions at $\sqrt{s}$ = 1.96 TeV*, *Phys. Rev. Lett.* **103** (2009) 101803 [0907.1269].

[40] CMS collaboration, *Search for a light charged Higgs boson in top quark decays in pp collisions at $\sqrt{s}$ = 7 TeV*, *JHEP* **07** (2012) 143 [1205.5736].

[41] ATLAS collaboration, *Search for charged Higgs bosons through the violation of lepton universality in t$\bar{t}$ events using pp collision data at $\sqrt{s}$ = 7 TeV with the ATLAS experiment*, *JHEP* **03** (2013) 076 [1212.3572].

[42] ATLAS collaboration, *Search for charged Higgs bosons decaying via $H^{\pm} \to \tau^{\pm}\nu$ in top quark pair events using pp collision data at $\sqrt{s}$ = 7 TeV with the ATLAS detector*, *JHEP* **06** (2012) 039 [1204.2760].

[43] ATLAS collaboration, *Search for charged Higgs bosons decaying via $H^{\pm} \to \tau^{\pm}\nu$ in fully hadronic final states using pp collision data at $\sqrt{s}$ = 8 TeV with the ATLAS detector*, *JHEP* **03** (2015) 088 [1412.6663].

[44] CMS collaboration, *Search for a light charged Higgs boson decaying to $c\bar{s}$ in pp collisions at $\sqrt{s}$ = 8 TeV*, *JHEP* **12** (2015) 178 [1510.04252].

[45] CMS collaboration, *Search for a light charged Higgs boson in the $H^{\pm} \to cs$ channel in proton-proton collisions at $\sqrt{s}$ = 13 TeV*, *Phys. Rev. D* **102** (2020) 072001 [2005.08900].

[46] CMS collaboration, *Search for a charged Higgs boson decaying to charm and bottom quarks in proton-proton collisions at $\sqrt{s}$ = 8 TeV*, *JHEP* **11** (2018) 115 [1808.06575].

[47] ATLAS collaboration, *Search for a light charged Higgs boson in the decay channel $H^{+} \to c\bar{s}$ in t$\bar{t}$ events using pp collisions at $\sqrt{s}$ = 7 TeV with the ATLAS detector*, *Eur. Phys. J. C* **73** (2013) 2465 [1302.3694].

[48] ATLAS collaboration, *Search for a light charged Higgs boson in $t \to H^{\pm}b$ decays, with $H^{\pm} \to cb$, in the lepton+jets final state in proton-proton collisions at $\sqrt{s}$ = 13 TeV with the ATLAS detector*, 2302.11739.

[49] ALEPH, DELPHI, L3, OPAL, LEP collaboration, *Search for Charged Higgs bosons: Combined Results Using LEP Data*, *Eur. Phys. J. C* **73** (2013) 2463 [1301.6065].

[50] CMS collaboration, *Search for a light charged Higgs boson decaying to a W boson and a CP-odd Higgs boson in final states with e$\mu\mu$ or $\mu\mu\mu$ in proton-proton collisions at $\sqrt{s}$ = 13 TeV*, *Phys. Rev. Lett.* **123** (2019) 131802 [1905.07453].

[51] CMS collaboration, *Search for a charged Higgs boson decaying into a heavy neutral Higgs boson and a W boson in proton-proton collisions at $\sqrt{s}$ = 13 TeV*, 2207.01046.

[52] ATLAS collaboration, *Search for $H^{\pm} \to W^{\pm}A \to W^{\pm}\mu\mu$ in $pp \to t\bar{t}$ events using an $e\mu\mu$ signature with the ATLAS detector at $\sqrt{s}$ = 13 TeV* , ATLAS-CONF-2021-047.

[53] P. Bechtle, D. Dercks, S. Heinemeyer, T. Klingl, T. Stefaniak, G. Weiglein et al., *HiggsBounds-5: Testing Higgs Sectors in the LHC 13 TeV Era*, *Eur. Phys. J. C* **80** (2020) 1211 [2006.06007].

[54] P. Bechtle, S. Heinemeyer, T. Klingl, T. Stefaniak, G. Weiglein and J. Wittbrodt, *HiggsSignals-2: Probing new physics with precision Higgs measurements in the LHC 13 TeV era*, *Eur. Phys. J. C* **81** (2021) 145 [2012.09197].

[55] F. Mahmoudi, *SuperIso v2.3: A Program for calculating flavor physics observables in Supersymmetry*, *Comput. Phys. Commun.* **180** (2009) 1579 [0808.3144].

[56] M. Guchait and S. Moretti, *Improving the discovery potential of charged Higgs bosons at Tevatron run II*, *JHEP* **01** (2002) 001 [hep-ph/0110020].

[57] S. Moretti, *Pair production of charged Higgs scalars from electroweak gauge boson fusion*, *J. Phys. G* **28** (2002) 2567 [hep-ph/0102116].

[58] A. Belyaev, N.D. Christensen and A. Pukhov, *CalcHEP 3.4 for collider physics within and beyond the Standard Model*, *Comput. Phys. Commun.* **184** (2013) 1729 [1207.6082].

[59] D.J. Miller, S. Moretti, D.P. Roy and W.J. Stirling, *Detecting heavy charged Higgs bosons at the CERN LHC with four b quark tags*, *Phys. Rev. D* **61** (2000) 055011 [hep-ph/9906230].

[60] S. Moretti, K. Odagiri, P. Richardson, M.H. Seymour and B.R. Webber, *Implementation of supersymmetric processes in the HERWIG event generator*, *JHEP* **04** (2002) 028 [hep-ph/0204123].

[61] A. Djouadi, J. Kalinowski and P.M. Zerwas, *Two and three-body decay modes of SUSY Higgs particles*, *Z. Phys. C* **70** (1996) 435 [hep-ph/9511342].

[62] T.G. Rizzo, *Decays of Heavy Higgs Bosons*, *Phys. Rev. D* **22** (1980) 722.

[63] R.N. Cahn, *The Higgs Boson*, *Rept. Prog. Phys.* **52** (1989) 389.

[64] W.R. Inc., "Mathematica, Version 13.2."

[65] A.G. Akeroyd, S. Moretti and M. Song, *Slight excess at 130 GeV in search for a charged Higgs boson decaying to a charm quark and a bottom quark at the Large Hadron Collider*, *J. Phys. G* **49** (2022) 085004 [2202.03522].

[66] A.G. Akeroyd, *Three body decays of Higgs bosons at LEP-2 and application to a hidden fermiophobic Higgs*, *Nucl. Phys. B* **544** (1999) 557 [hep-ph/9806337].

[67] J.F. Gunion and H.E. Haber, *The CP conserving two Higgs doublet model: The Approach to the decoupling limit*, *Phys. Rev. D* **67** (2003) 075019 [hep-ph/0207010].

[68] H.E. Haber, *The Higgs data and the Decoupling Limit*, in *1st Toyama International Workshop on Higgs as a Probe of New Physics 2013*, 12, 2013 [1401.0152].

[69] D.M. Asner et al., *ILC Higgs White Paper*, in *Snowmass 2013: Snowmass on the Mississippi*, 10, 2013 [1310.0763].

[70] N.A. Graf, M.E. Peskin and J.L. Rosner, eds., *Proceedings, 2013 Community Summer Study*

on the Future of U.S. Particle Physics: Snowmass on the Mississippi (CSS2013): Minneapolis, MN, USA, July 29-August 6, 2013, 2013.